VLF electromagnetic field structures in ionosphere disturbed by Sura RF heating facility

V. O. Rapoport,[1] V. L. Frolov,[1] S. V. Polyakov,[1] G. P. Komrakov,[1] N. A. Ryzhov,[1] G. A. Markov,[2] A. S. Belov,[2] M. Parrot,[3] and J.-L. Rauch[3]

Received 19 March 2010; revised 27 May 2010; accepted 29 June 2010; published 26 October 2010.

[1] Observation of spatial VLF field structures in an artificially disturbed ionosphere is reported. The disturbed area with horizontal sizes ~50 km in a quiet middle-latitude ionosphere was produced by the powerful RF Sura heating facility (56°1′N, 46°1′E). Measurements were carried out onboard the DEMETER satellite while passing the disturbed area at height ~700 km. Spectra broadening ($\Delta f < \pm 1$ kHz) and considerable (up to 30 dB) increase of signal intensity of VLF transmitters' signals were observed. The VLF field and electron density irregularities have similar spatial structure. The characteristics of the VLF field in disturbed by RF heating area are analyzed.

Citation: Rapoport, V. O., V. L. Frolov, S. V. Polyakov, G. P. Komrakov, N. A. Ryzhov, G. A. Markov, A. S. Belov, M. Parrot, and J.-L. Rauch (2010), VLF electromagnetic field structures in ionosphere disturbed by Sura RF heating facility, *J. Geophys. Res.*, *115*, A10322, doi:10.1029/2010JA015484.

1. Introduction

[2] Active experiments in ionosphere and magnetosphere have been carried out since the 1970s [*Storey*, 1953; *Helliwell*, 1969; *Helliwell*, 1988; *Gurevich*, 2007].

[3] It is believed that VLF signals from powerful ground-based transmitters determines the lifetime of energetic radiation belt electrons (100 keV–1.5 MeV) on L-shells in the range of 1.3–2.8 [*Abel and Thorne*, 1998a; *Abel and Thorne*, 1998b; *Millan and Thorne*, 2007]. Moreover the authors of [*Abel and Thorne*, 1998a; *Abel and Thorne*, 1998b; *Koon et al*, 1981; *Imhof et al*, 1983] concluded that man-made VLF transmitters operating continuously in the 17–23 kHz range have a significant impact on 100–1500 keV electron lifetimes. The studies of transmitter-induced precipitation (e.g., *Inan et al.*, 1984) have concentrated on magnetospherically "ducted" propagation, placing the predicted precipitation regions in the vicinity of the major transmitters, largely located at L-shells of L > 2. To test the hypothesis that VLF signals from ground-based transmitters determine the lifetimes of energetic radiation belt electrons, one needs to know the characteristics of the VLF signals in the radiation belts. In turn, the intensity of VLF signal is determined substantially by the structure of ionosphere-magnetosphere plasma.

[4] Usually it is believed that only large-scale irregularities elongated along the magnetic field (ducts) can influence the wave propagation into the ionosphere and magnetosphere [*Helliwell*, 1969; *Helliwell*, 1988; *Inan*, 1987; *Milikh et al.*, 2008; *Poulsen et al.*, 1990; *Smith et al.*, 1960]. However there is an alternative that small-scale irregularities (~100 m and over) also play a significant role in wave propagation. In this case the wave-scattering on irregularities with a mode transition is a significant phenomenon determining the characteristics of VLF waves in upper ionosphere and magnetosphere.

[5] Irregular structure of VLF field and increase of its intensity in inhomogeneous ionosphere was observed in numerous DEMETER satellite measurements in the auroral region [*Titova et al.*, 1984a; *Titova et al.*, 1984b; *Trakhtengerts and Titova*, 1985; *Basu*, 1978; *Reid*, 1968; *Sudan et al.*, 1973; *Villain et al.*, 1985, *Sonwalkar et al.*, 2001; *Baker et al.*, 2000; *Groves et al.*, 1988; *Seyler*, 1990]. The increase of VLF field intensity was accompanied by a spectral broadening while the satellite crosses the area with inhomogeneous medium. The effect of VLF wave spectrum broadening was also observed in satellite measurements of artificial ionosphere perturbations created by RF heating facilities [*Bell et al.*, 2008; *Rapoport et al.*, 2007]. Moreover the effect was observed only in the heated area and ceased when the satellite left the area.

[6] The broadening of VLF signals' spectra could be interpreted by a whistler wave transformation into quasi-longitudinal (electrostatic) mode. [*Bell and Ngo*, 1990; *Bell and Ngo*, 1988; *Trakhtengerts et al.*, 1996; *Bell et al.*, 2008]. The lower hybrid (quasi-longitudinal) waves are excited as the electromagnetic whistler mode wave scatter from magnetic-field-aligned plasma density irregularities in the ionosphere and magnetosphere. Calculations of wave scattering on small-scale irregularities with whistler to electrostatic mode transformation were performed by *Bell and Ngo* [1990]. The spectrum width of lower hybrid waves in the process is determined by the irregularity's spatial spectrum and is comparable with it.

[7] Unlike the wave scattering on small-scale irregularities the process of VLF wave propagation in duct has a

[1]Radiophysical Research Institute, Nizhniy Novgorod, Russia.
[2]Nizhniy Novgorod State University, Nizhniy Novgorod, Russia.
[3]Laboratorie de Physique et Chimie de l'Environnement et de l'Espace/CNRS, Orléans, France.

0148-0227/10/2010JA015484

Table 1. Experimental Characteristics of 1 May 2006 and 17 May 2006 Experiments

	1 May 2006 Experiment	*17 May 2006 Experiment*
Time of the closest approach of the satellite to the center of the perturbed region (UT)	18:28:38	18:28:30
The minimum distance from the satellite to the center of the disturbed magnetic tube	35 km	39 km
Pumping wave frequency	4300 kHz	4785 kHz
Pumping wave effective power	80 MW	120 MW
Inclination of SURA facility antenna beam	12° to the south	12° to the south
Ionosphere cutoff frequency, $f_0(F_2)$	5.8 MHz	5.9 MHz
Pumping wave reflection height	230 km	220 km
K_p index	0^+	0
Special conditions	E_s diffusivity up to 3.8 MHz	

narrow spectrum. Under the eikonal approximation the angle between wave vector and magnetic field is determined by Snell's law. It is approximately equal to the relative electron density perturbation and is no larger than 0.1–0.2. Thus the transversal component of the wave vector must be considerably smaller than longitudinal one in the process of wave trapping into the duct. Analysis of wave propagation in artificially created waveguides was performed by *Karpman and Kaufman* [1982]. The eigenvalue and eigenvectors of waves propagating in such a waveguide are given by *Yoom et al.* [2007].

[8] In our experiments discussed below the VLF wave intensity increased sharply and its spectrum broadened while the satellite crossed the disturbed area. This assumes that the wave-scattering on small-scale irregularities with a mode transition is realized in the experiments.

[9] The subject of the present paper concerns the characteristics of the VLF signals at 18.1 kHz as observed on the DEMETER spacecraft at 710 km altitude, see special issue of Planetary and Space Science, Parrot, M. (2006), "DEMETER," *Planet. Space Sci.*, *54*, 411.

[10] The analysis of the VLF waves' propagation in the area with artificially created irregularities allows us to match the data on transversal scales of waves with a theoretical model's characteristics (such as dispersion characteristics, impedance, etc.).The VLF signals spectral features permits the supposition that the process of energy transfer between the whistler end electrostatic mode occurs and could be described as diffusion in k-space.

[11] In our experiments, the heating of the ionospheric plasma has been performed by the powerful RF Sura facility. The DEMETER satellite was used for diagnostics of ionospheric parameters and electromagnetic waves [*Rapoport et al.*, 2007; *Frolov et al.*, 2007].

2. Experiment Results

[12] Measurements of VLF wave fields and plasma parameters in the ionosphere disturbed by RF Sura heating facility were carried out by the DEMETER satellite [*Rapoport et al.*, 2007; *Frolov et al.*, 2007]. The experiments were carried out in the evening (22 LT) on 1 May 2006 and 17 May 2006. The height of the satellite orbit was 710 km, and the satellite velocity was ~7.7 km s^{-1}. The Sura facility operated during 15 min in CW (ordinary polarized wave) mode creating an artificial ionosphere turbulence. The minimum distance between the satellite and the center of the perturbed area was approximately 35–40 km.

[13] The characteristics of the satellite instruments are presented in a special issue of *Planetary and Space Science*, Parrot, M. (2006), "DEMETER," *Planet. Space Sci.*, *54*, 411.

[14] The DEMETER plasma wave instrument (ICE) [*Berthelier et al.*, 2006] was used to detect the VLF (up to 20 kHz) and quasi-static electric field (frequency range 0–1.25 kHz). Langmuir probe [*Lebreton et al.*, 2006] was used to measure electron density and the Magnetic Search Coil (IMSC) instrument [*Parrot et al.*, 2006] for magnetic field measurements. The satellite measurements were carried out in *Burst mode*, under which the electron and ion density and

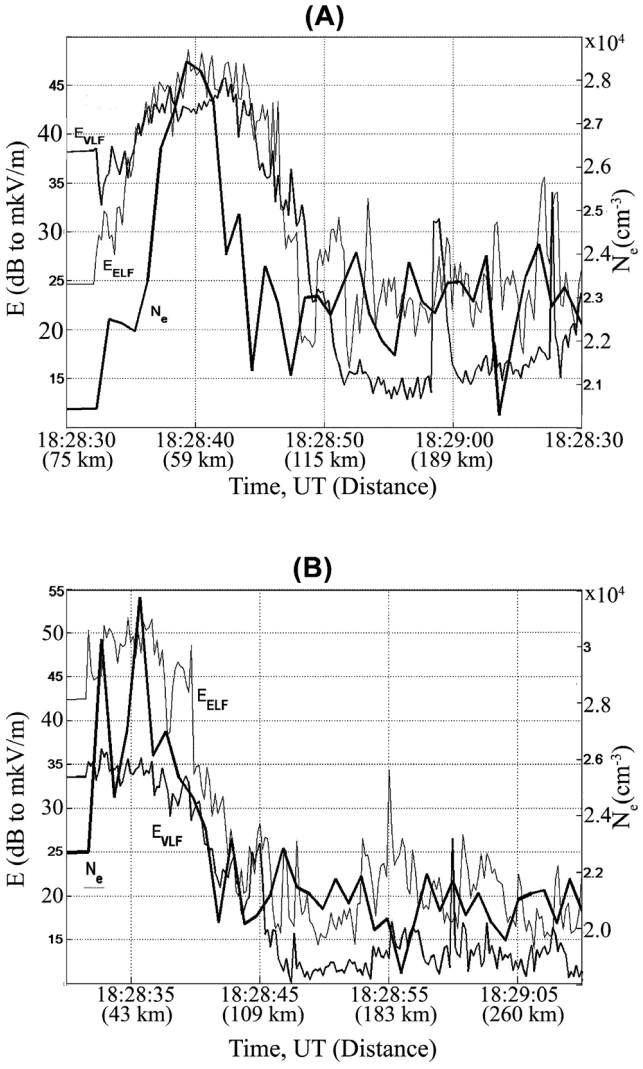

Figure 1. Electron density (N_e), VLF electric field (E_{VLF}, frequency range of 17.6–19.1 kHz), and quasi-static electric field (E_{ELF}, frequency range of 0–1 kHz) as a function of the distance (in brackets) up to the center of the disturbed region of field tube (the heated area). Figure 1a is related to the 1 May 2006 session whereas Figure 1b corresponds to the 17 May 2006 session.

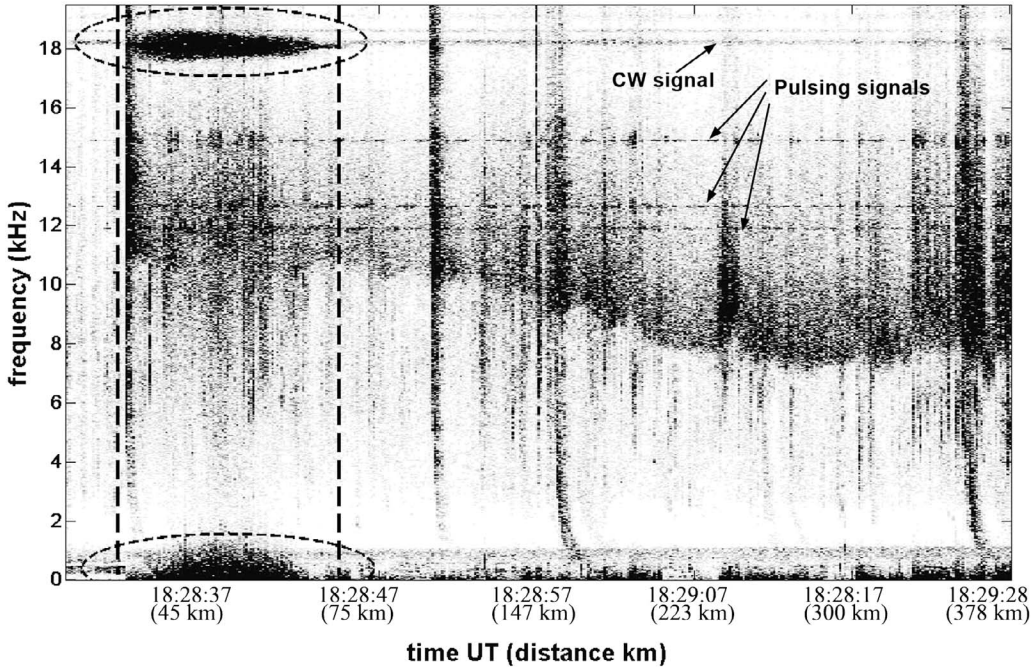

Figure 2. The electric field frequency-time spectrogram for 1 May 2006 session. Vertical lines mark the time of DEMETER flight through the heated area. Signals of VLF stations (continuous wave and pulsing) are marked with arrows. The boundary at 8–11 kHz corresponds to LHR frequency.

the temperatures of the plasma component were registered with a time resolution of about 1 s. The sampling frequency of electric and magnetic field detectors was 40,000 samples per second. Ionosphere cutoff frequency $f_0(F_2)$ and the main parameters of the Sura facility during the experiment's sessions are given in Table 1.

[15] Figure 1a shows an electron density (N_e), intensity of the VLF electric field in a frequency range of 17.6–19.1 kHz (E_{VLF}), and the intensity of the quasi-static electric field in a range of 0–1 kHz (E_{ELF}) over a 40 s time period for the 1 May 2006 session. These data were acquired near the magnetic field line intersecting the heating area of the Sura facility. Figure 1b is the same for the 17 May 2006 session. In both sessions, the beginning of measurements in *Burst mode* was at 18:28:32 UT (22:28:32 LT).

[16] From Figures 1a and 1b one can see that at the closest approach to the center of the heated area both electron density of plasma and electric field intensity increase. The size of the perturbed electron density area is estimated as $L_N \simeq 45$ km since time of satellite flight in the disturbed region in about 6–7 s. The size of the increased electric field area is about $L_E \simeq 90$–100 km and outside this area the intensity of the VLF field decreases abruptly by ~30 dB.

[17] The frequency-time spectrogram of VLF electric field in a frequency range of 0–19.5 kHz is shown on Figure 2. This spectrogram is given for the 1 May 2006 experiment session between 18:28:32 and 18:29:28 UT (distances to the center of the heated area are in brackets). Several VLF transmitter signals were detected—a continuous wave (CW) signal at a frequency close to 18 kHz and a pulsing signal at frequencies close to 12, 13, and 15 kHz. Ovals mark the frequency broadening of CW VLF signal and quasi-static noise caused by artificial ionosphere irregularities in the heated area.

[18] In the heated area of the ionosphere which DEMETER flew through at 18:28:33–18:28:45 UT (marked with vertical lines) the intensity of CW VLF signal at 18 kHz significantly increases together with its spectrum width. Signal bandwidth for this transmitter is as large as 1 kHz during this period. Spectra of pulsing VLF signals also broadened in the areas with artificial ionosphere irregularities.

[19] Figure 3 shows the sequence of electric and magnetic fields' power spectra measured in the disturbed area in a frequency range of 17.5–18.7 kHz. On each spectrum, the electric field is shown by a thin line (the left scale of intensity, dB to 1 $\mu V/m\ Hz^{1/2}$), and magnetic field is represented by a bold line (the right scale of intensity, dB to $1nT/Hz^{1/2}$). To compute spectra we used series of 10 data arrays of 0.2 s duration (spectral resolution ~5 Hz) and then averaged these power spectra.

[20] As one can see from Figure 3, the spectrum of the VLF electric field consists of two components: a quasi-monochromatic line at the VLF transmitter's pumping wave frequency (18.1 kHz) and a noise continuum with a maximum at the same frequency and a bandwidth of about 0.4–0.5 kHz (at a 3 dB level). The noise continuum level increases up to 30 dB in a bandwidth of ±0.3 kHz. At distances up to 60 km from the center of disturbed area the carrier frequency is masked by the noise level. At distances of 60–100 km the intensity of pumping frequency signal did not change, while the intensity of the noise continuum monotonously decreases. At distances of 100–130 km the signal decreases abruptly (by 30 dB).

[21] Figure 4 shows the power spectra for the electrostatic field (a continuous line for a frequency range of 0–1 kHz) and for the noise VLF continuum (2, 3). Here the VLF frequency is counted both up and down from the pumping frequency (18.1 kHz). The dashed curve corresponds to the

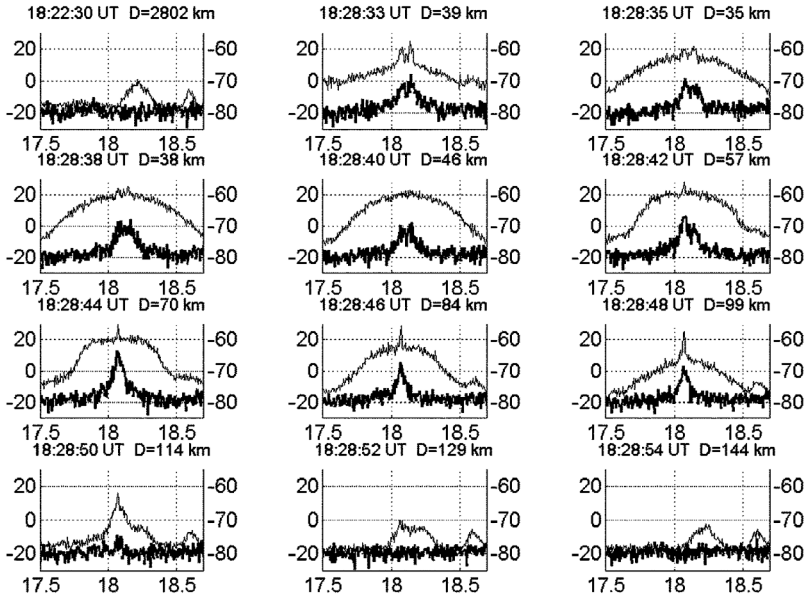

Figure 3. The sequence of averaged power spectra for VLF electric and magnetic fields in an interval of frequencies 17.5–18.7 kHz for the consecutive moments of time and distances of satellite up to the center of the field tube of the heated area. The distance (km) from the satellite up to the center of the field tube and the time (UT) are shown above each spectrum. The intensity spectral density of electric field is shown by a thin line (the left scale of intensity, dB to 1 $\mu V^2/m^2\ Hz$), the spectral density of a magnetic field is given by a bold line (the right scale of intensity, dB to nT^2/Hz).

interval of frequencies of 18.1–19.1 kHz, and the dotted curve to an interval of frequencies 18.1–17.1 kHz.

[22] The frequency dependence of a continuum spectral intensity $E(f)$ may be defined as a power law $E^2 \sim f^{\alpha}$. In this case, the change of the spectral intensity could be characterized by a spectral index $\alpha = \log_{10}(E_1^2/E_2^2)/\log_{10}(f_2/f_1)$. The spectral index of the quasi-static electric field is about $\alpha \simeq -2.6$ in a frequency range of 30–1000 Hz (Figure 4). The spectral index of the VLF continuum is $\alpha \simeq 0$ in a frequency range of 30–150 Hz, and at frequencies from 150 to 300 Hz it is $\alpha \simeq -2.6$. At frequencies above 300 Hz spectral intensity of the VLF continuum sharply decreases ($\alpha \simeq -5.5$). The spectra of the VLF signal for positive (18.1–19.1 kHz) and negative (18.1–17.1) frequencies from the central frequency are similar (Figures 3 and 4).

3. Discussion

[23] A solitary large-scale electron density irregularity with the size of ~40 km was observed above the heated area. The electron density within this irregularity exceeds the background level by 10%–20%.

[24] We can assume that the small-scale irregularities of electron density have the same scales as electrostatic field. Taking into account the satellite velocity, the electrostatic field was recorded by satellite probes at frequencies 10 Hz–1 kHz, and this corresponds to spatial scales of $l \sim \omega v_{sat}/2\pi \sim (1000 \div 10)$ meters.

[25] As it follows from Figure 1, the area of increased electric field largely coincides with the electron density disturbance area, which has a noticeably large size. The VLF field abruptly decreases outside the heated area confirming the guiding of VLF waves into the upper ionosphere. It is apparent that waves do not propagate in a duct, but more likely as waves which "move" along the small-scale irregularities of the electron density (duct is understood as a waveguide with the cross-section more than wavelength).

[26] In order to study the VLF spatial spectrum features we consider the spatial distribution of the VLF field irregularities and their connection with dispersion characteristics of the field. For whistlers with

$$\omega_{LHR} \ll \omega \ll \omega_{He}, \omega_{0e}, \tag{1}$$

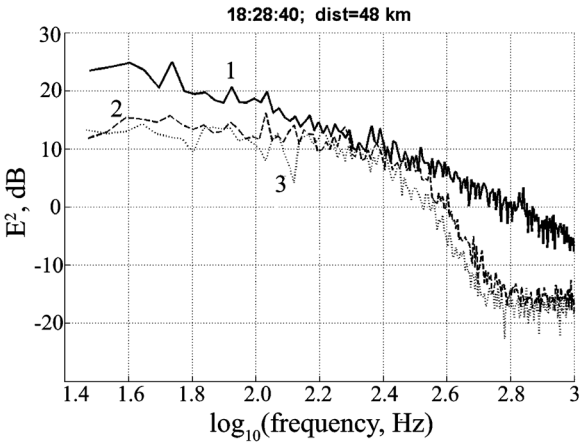

Figure 4. The power spectra of an electric signal for the electrostatic field—a continuous line for the frequency range of 0–1 kHz (1), and for a noise VLF continuum: dashed line—in a frequency range of 18.1–19.1 kHz (2), dotted line—in a frequency range of 18.1–17.1 kHz (3). (dB to $\mu V/m\ Hz^{1/2}$).

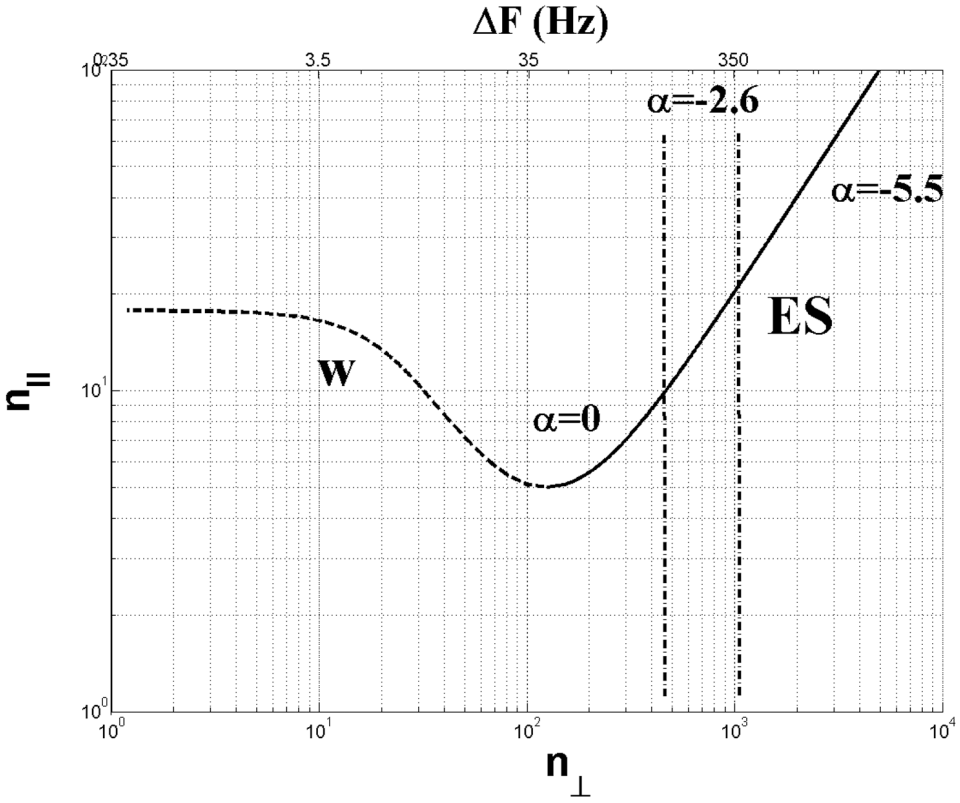

Figure 5. Dispersive curve $n_{\|}(n_{\perp})$ for VLF waves ($\omega_{0e}/\omega_{He} = 2.5$, $\omega/\omega_{He} = 0.02$).

(where ω is frequency of the VLF waves, ω_{He} and ω_{0e} are electron gyrofrequency and plasma frequency, respectively, and ω_{LHR} the lower hybrid resonance frequency), all components of dielectric permeability tensor are proportional to the electron density [*Karpman and Kaufman*, 1982]. The dispersion equation for the VLF waves with the condition (1) is as follows *Karpman and Kaufman* [1983a and 1983b] and:

$$n_{\perp}^2 = \left(2u^2\right)^{-1}\left[\left(1-2u^2\right)n_{\|}^2 - 2a \pm \sqrt{n_{\|}^4 - 4an_{\|}^2}\right], \qquad (2)$$

(where $k_0 = \omega/c$ is the wave number in vacuum, $a = \omega_{0e}^2/\omega_{He}^2$, $u = \omega/\omega_{He}$).

[27] Here instead of wave number $\mathbf{k}$ the parameters $\mathbf{n} = \mathbf{k}/k_0$ with components $n_{\|}$ (along a magnetic field) and $n_{\perp}$(across a magnetic field) are used. The sign "–" before the square root corresponds to the whistler mode (W), and the sign "+" corresponds to the electrostatic mode (ES). There is an interval of $n_{\|}$ in which both modes exist simultaneously. The dispersion curve $n_{\|}(n_{\perp})$ for the case $\omega_{0e}/\omega_{He} = 2.5$, $\omega/\omega_{He} = 0.02$ (which corresponds to middle-latitude ionosphere parameters at height of ~700 km, and for a VLF signal frequency ~20 kHz) is shown on Figure 5. The dotted part of the curve on Figure 5 corresponds to the whistler mode (W), and the continuous part of the curve to the electrostatic mode (ES).

[28] Time dependence of the satellite data records is connected with the spatial structure of the field by the expression:

$$E_{sat}(t) = e^{-i\omega_0 t}E(\mathbf{r}_0 - \mathbf{v}_{sat}t). \qquad (3)$$

($E(\mathbf{r})$ is the amplitude of the VLF field along the trajectory of the satellite, $\mathbf{r}_0$ are the coordinates of the satellite at $t = 0$). The frequency shift (ΔF) is defined by the expression $\Delta F = \mathbf{k}_{irreg}\ \mathbf{v}_{sat}/2\pi$ (where l_{irreg} - is the scale of irregularities, $|\mathbf{k}_{irreg}| = 2\pi/l_{irreg}$ is the "wave number" of irregularities). In our case (for values $a = \omega_{0e}^2/\omega_{He}^2 = 6.25$, and $u = \omega/\omega_{He} = 0.02$), the relation between frequency shift and $n_{\perp}$ is given by $\Delta F \approx 0.35 n_{\perp}$.

[29] Scattering of the electrostatic electric field (ES) to whistler (W) or of the electromagnetic whistlers (W) to electrostatic electric field (ES) from pre-existing density irregularities should be satisfied by synchronism conditions:

$$\mathbf{k_W} - \mathbf{k_{ES}} = \mathbf{k}_{irreg}, \qquad (4)$$

where k_{irreg} is the wave vector of electron density irregularities. These irregularities are elongated along the geomagnetic field. i.e., their spatial spectrum width along the geomagnetic field has a narrow wavelength range. $\mathrm{k}_{\|,irreg} \ll \mathrm{k}_{\|,W}, \mathrm{k}_{\|,ES}$. Thus, in the analysis a small parameter $\mu = \Delta k_{\|}/k_{\|}$ appears.

[30] Figure 6 shows the scattering from one mode to the other by arrows (solid arrows for scattering from whistler mode to electrostatic one, and dotted arrows in the reverse direction). Each act of wave scattering is accompanied by a change of $k_{\|}$ at the value $\Delta k_{\|} \sim \mathrm{k}_{\|,irreg}$.

[31] The presence of small parameter μ allows considering the VLF spatial spectra evolution as "diffusion" of wave in k-space along the longitudinal wave vector component ($k_{\|}$). Such "diffusion" may occur in the part on the dispersion curve where both modes (whistler and electrostatic)

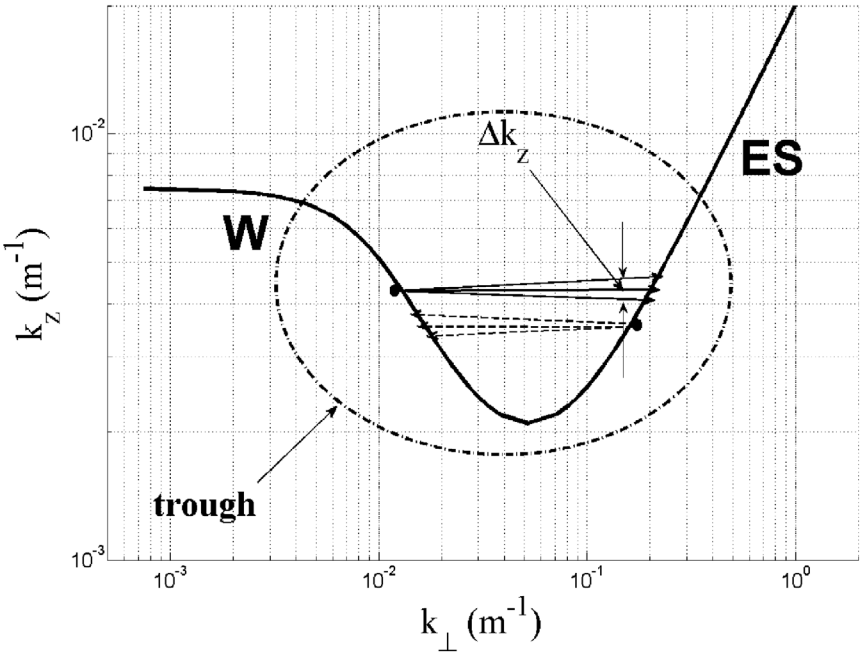

Figure 6. Wave scattering by ionosphere irregularities with mode transformation.

exist simultaneously. Figure 7 shows the distribution of the electric field intensity along the dispersion curve. Figure 7 represents a three-dimensional diagram combining the data from Figures 4 and 5. The spectral density of the electric field is more or less constant within the trough and drastically reduces on exit from it.

[32] An important parameter of radio wave propagation is admittance function (the ratio of the magnetic induction B to the electric field E) and its dependence from the spatial structure of the field. The relation follows from the Maxwell equation $[\mathbf{k}\,\mathbf{E}] - \omega\mathbf{B} = 0$ and the dispersion equation (2) as:

$$\frac{B}{E} = \frac{n_{\parallel}}{c} \frac{\omega_{0e}^2/\omega^2}{\sqrt{n_{\perp}^2 n_{\parallel}^2 + \left(n_{\perp}^2 + \omega_{0e}^2/\omega^2\right)^2}} \tag{5}$$

[33] The dotted curve on Figure 8 shows the calculated admittance (5) for the same parameters (ω_{0e}/ω_{He} = 2.5,

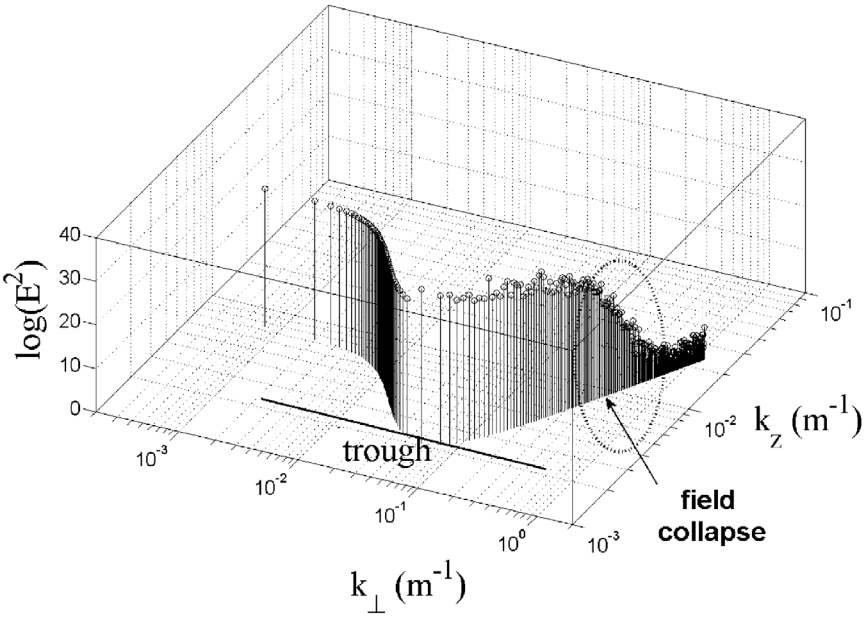

Figure 7. Distribution of the electric field intensity along the dispersive curve.

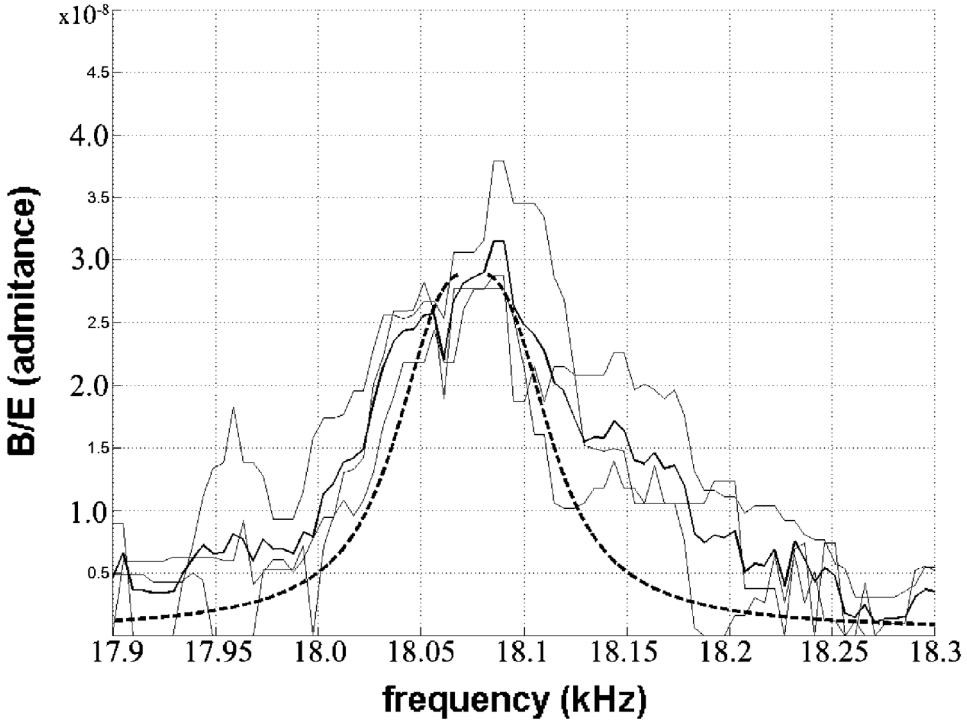

Figure 8. Comparison between the calculated admittance (a dotted curve; $\omega_{0e}/\omega_{He} = 2.5$, $\omega/\omega_{He} = 0.02$) and a set of experimental data curves of B/E.

$\omega/\omega_{He} = 0.02$) as for the dispersion curve (Figure 5). Figure 8 also represents B/E ratio obtained from experimental data. Thin lines shows the B/E values corresponding to spectra similar to spectra shown on Figure 3 for distances 49 km, 61 km, and 75 km. The darker line corresponds to averaged values. As it is evident from Figure 8, there is a good correspondence between theoretical calculation and experimental data.

[34] To summarize, a spectrum broadening effect and an increase of the VLF signal scattered by ionosphere irregularities was observed only in the disturbed area and was totally absent outside it. Experimental values of the admittance are in agreement with the calculated ones.

[35] It is believed that similar processes (wave scattering accompanied by the mode interaction) may occur in other frequency ranges. Specifically, such scattering may occur in the ULF range, where the transformation of magneto-acoustical waves into Alfvén waves, as well as in HF range in the interval of frequencies between the upper hybrid frequency and the plasma frequency. In all these cases a sufficiently effective scattering of waves of one mode into another may take place on small-scale irregularities of electron density

4. Conclusions

[36] The main conclusions are:

[37] 1. Above the HF heated area waves propagate not in duct (a waveguide with the cross–section more than wavelength), but more likely as waves that "move" along the small-scale irregularities in turbulent medium.

[38] 2. Interaction of whistler and electrostatic waves leads to "filling" of the trough on the dispersive curve ($k_{||}(k_{\perp})$ dependence).

[39] 3. A spatial spectrum of VLF waves has a flat part (whistler mode and the beginning of electrostatic mode), a part with a spectral index of −2.6 (a short-wave part of an electrostatic mode). Outside the trough, the signal is practically absent.

[40] **Acknowledgments.** This work is based on observations with experiments embarked on the micro-satellite DEMETER operated by the CNES. The authors thank J. J. Berthelier the PI of the electric field experiment and J. J. Lebreton the PI of the Langmuir probe for the use of the data. The work has been carried out with financial support of the Russian Foundation for Basic Research (grants 08-02-00171 and 09-05-00780).

[41] Robert Lysak thanks Jean-Andre Sauvaud and another reviewer for their assistance in evaluating this paper.

References

Abel, B., and R. M. Thorne (1998a), Electron scattering loss in the Earth's inner magnetosphere: 1. Dominant physical processes, *J. Geophys. Res.*, *103*, 2385. (Correction, J. Geophys. Res., 104, 4627, 1999).

Abel, B., and R. M. Thorne (1998b), Electron scattering loss in the Earth's inner magnetosphere: 2. Sensitivity to model parameters, *J. Geophys. Res.*, *103*, 2397. (Correction, J. Geophys. Res., 104, 4627, 1999).

Baker, S. D., M. C. Kelley, C. M. Swenson, J. Bonnell, and D. V. Hahn (2000), Generation of electrostatic emissions by lightning-induced whistler-mode radiation above thunderstorms, *J. Atmos. Sol.Terr. Phys.*, *62*(15), 1393–1404.

Basu, S. (1978), Ogo 6 observations of small-scale irregularity structures associated with subtrough density gradients, *J. Geophys. Res.*, *83*(A1), 182–190.

Bell, T., and H. Ngo (1988), Electrostatic waves stimulated by coherent VLF signals propagating in and near the inner radiation belt, *J. Geophys. Res.*, *93*(A4), 2599–2618.

Bell, T. F., and H. D. Ngo (1990), Electrostatic lower hybrid waves excited by electromagnetic whistler mode waves scattering from planar magnetic-

field-aligned plasma density irregularities, *J. Geophys. Res.*, *95*(A1), 149–172.

Bell, T. F., U. S. Inan, D. Piddyachiy, P. Kulkarni, and M. Parrot (2008), Effects of plasma density irregularities on the pitch angle scattering of radiation belt electrons by signals from ground based VLF transmitters, *Geophys. Res. Lett.*, *35*, L19103, doi:10.1029/2008GL034834.

Berthelier, J. J., et al. (2006), ICE, The electric field experiment on DEMETER, *Planet. Space Sci.*, *54*, 456–471.

Frolov, V. L., et al. (2007), Modification of the earth's ionosphere by high-power high-frequency radio waves, *Phys. Usp.*, *50*(3), 315–324.

Groves, K., M. Lee, and S. Kuo (1988), Spectral broadening of VLF radio signals traversing the ionosphere, *J. Geophys. Res.*, *93*(A12), 14,683–14,687.

Gurevich, A. V. (2007), Nonlinear effects in the ionosphere, *Phys. Usp.*, *50*(11), 1091–1121.

Helliwell, R. A. (1969), Low-frequency waves in the magnetosphere, *Rev. Geophys.*, *7*(1,2), 281–303.

Helliwell, R. A. (1988), VLF wave stimulation experiments in the magnetosphere from Siple Station, Antarctica, *Rev. Geophys.*, *26*(3), 551–578.

Inan, U. S. (1987), Waves and instabilities, *Rev. Geophys.*, *25*(3), 588–598.

Inan, U., H. Chang, and R. Helliwell (1984), Electron precipitation zones around major ground-based VLF signal sources, *J. Geophys. Res.*, *89*(A5), 2891–2906.

Imhof, W. L., J. B. Reagan, H. D. Voss, E. E. Gaines, D. W. Datlowe, J. Mobilia, R. A. Helliwell, U.S. Inan, J. Katsufrakis, and R. G. Joiner (1983), The modulated precipitation of radiation belt electrons by controlled signals from ground-based transmitters, *Geophys. Res. Lett.*, *10*, 615.

Karpman, V. I., and R. N. Kaufman (1982), Whistler wave propagation in density ducts, *J. Plasma Phys.*, *27*(02), 225–238.

Karpman, V. I., and R. N. Kaufman (1983a), Peculiarities of whistler wave's propagation in magnetosphere ducts in subequatorial area. I. Ducts with increased density, *Geomagn. Aeron.*, *23*, 451–457.

Karpman, V. I., and R. N. Kaufman (1983b), Peculiarities of whistler wave's propagation in magnetosphere ducts in subequatorial area. II. Ducts with decreased density, *Geomagn. Aeron.*, *23*, 791–796.

Koon, H. C., B. C. Edgar, and A. L. Vampola (1981), Precipitation of inner zona electrons by whistler mode waves from the VLF transmitters UMS and NWC, *J. Geophys. Res.*, *86*(A2), 640–648.

Lebreton, J.-P., et al. (2006), The ISL Langmuir probe experiment processing onboard DEMETER: Scientific objectives, description and first results, *Planet. Space Sci.*, *54*, 472–486.

Milikh, G. M., K. Papadopoulos, H. Shroff, C. L. Chang, T. Wallace, E. V. Mishin, M. Parrot, and J. J. Berthelier (2008), Formation of artificial ionospheric ducts, *Geophys. Res. Lett.*, *35*, L17104, doi:10.1029/2008GL034630.

Millan, R. M., and R. M. Thorne (2007), Review of radiation belt relativistic electron losses, *J. Atmos. Sol.Terr. Phys.*, *69*, 362.

Parrot, M., et al. (2006), The magnetic field experiment IMSC and its data processing onboard DEMETER: Scientific objectives, description and first results, *Planet. Space Sci.*, *54*, 441–455, doi:10.1016/j.pss.2005.10.015.

Poulsen, W., T. Bell, and U. Inan (1990), Three-Dimensional modeling of subionospheric VLF propagation in the presence of localized D region perturbations associated with lightning, *J. Geophys. Res.*, *95*(A3), 2355–2366.

Rapoport, V. O., V. L. Frolov, G. P. Komrakov, G. A. Markov, A. S. Belov, M. Parrot, and J. L. Rauch (2007), Some results of measuring the characteristics of electromagnetic and plasma disturbances stimulated in the outer ionosphere by high-power high-frequency radio emission from the "Sura" facility, *Radiophysics Quantum Electri.*, *50*(8), 645–656.

Reid, G. (1968), The formation of small-scale irregularities in the ionosphere, *J. Geophys. Res.*, *73*(5), 1627–1640.

Seyler, C. (1990), A mathematical model of the structure and evolution of small-scale discrete auroral arcs, *J. Geophys. Res.*, *95*(A10), 17,199–17,215.

Smith, R. L., R. A. Helliwell, and I. W. Yabroff (1960), A theory of trapping of whistlers in field-aligned columns of enchanced ionization, *J. Geophys. Res.*, *65*(3), 815.

Sonwalkar, V. S., X. Chen, J. Harikumar, D. L. Carpenter, and T. F Bell. (2001), Whistler-mode wave-injection experiments in the plasmasphere with a radio sounder, *J. Atmos. Sol.Terr. Phys.*, *63*(11), 1199–1216.

Storey, L. R. O. (1953), An investigation of whistling atmospherics. *Phil. Trans. R. Soc. London, Ser. A*, *246*, 113–141.

Sudan, R., J. Akinrimisi, and D. Farley (1973), Generation of small-scale irregularities in the equatorial electrojet, *J. Geophys. Res.*, *78*(1), 240–248.

Titova, E. E., V. I. Di, V. E. Yurov, O. M. Raspopov, V. Yu. Trakhtengertz, F. Jiricek, and P. Triska (1984a), Interaction between VLF waves and the turbulent ionosphere, *Geophys. Res. Lett.*, *11*(4), 323–326.

Titova, E. E., V. I. Di, F. Jiricek, I. V. Lychkina, O. M. Raspopov, V. Yu. Trakhtengertz, P. Triska, and V. E. Yurov (1984b), VLF transmitters' spectra broadening in upper ionosphere, *Geomagn. Aeron.*, *24*(6), 935–943.

Trakhtengerts, V. Yu., and E. E. Titova (1985), Interaction of monochromatic VLF waves with the turbulent ionosphere, *Geomagn. Aeron.*, *25*(1), 89–96.

Trakhtengerts, V., M. Rycroft, and A. Demekhov (1996), Interrelation of noise-like and discrete ELF/VLF emissions generated by cyclotron interactions, *J. Geophys. Res.*, *101*(A6), 13,293–13,301.

Villain, J., G. Caudal, and C. Hanuise (1985), A Safari-Eiscat comparison between the velocity of F region small-scale irregularities and the ion drift, *J. Geophys. Res.*, *90*(A9), 8433–8443.

Yoom, P. H., S. Ye. LaBelle, A. T. Weatherwax, and J. D. Menietti (2007), Methods in the study of discrete upper hybrid waves, *J. Geophys. Res.*, *112*, A11305, doi:10.1029/2007JA012683.

Yurov, V. E. (1984), VLF transmitters' spectra broadening in upper ionosphere, *Geomagn. Aeron.*, *24*(6), 935–943.

A. S. Belov and G. A. Markov, Nizhniy Novgorod State University, Nizhniy Novgorod, Russia.

V. L. Frolov, G. P. Komrakov, S. V. Polyakov, V. O. Rapoport, and N. A. Ryzhov, Radiophysical Research Institute, Nizhniy Novgorod, Russia. (wrapoport@nirfi.sci-nnov.ru)

M. Parrot and J.-L. Rauch, Laboratorie de Physique et Chimie de l'Environnement et de l'Espace/CNRS, Orléans, France.